Contents lists available at SciOpen

Food Science and Human Wellness

journal homepage: https://www.sciopen.com/journal/2097-0765

China Food Publishing Co.

A fungal insoluble fiber from *Antrodia camphorata* modulates Ruminococcaceae and *Helicobacter* to restore lipid homeostasis *via* glycerophospholipid metabolism in HFD mice

Xin Song[a], Hui Li[a], Peng Meng[a], Guangqiang Wang[a], Fan Xie[a,b], Zhiqiang Xiong[a], Yijin Yang[a], Hui Zhang[a], Tingting Shen[c,*], Yongjun Xia[a,b,*], Lianzhong Ai[a,b]

[a] *Shanghai Engineering Research Center of Food Microbiology, School of Health Science and Engineering, University of Shanghai for Science and Technology, Shanghai 200093, China*
[b] *Department of Food Science & Technology, School of Agriculture and Biology, Shanghai Jiao Tong University, Shanghai 200240, China*
[c] *Department of Infectious Diseases, Tongren Hospital, Shanghai Jiao Tong University School of Medicine, Shanghai 200336, China*

ARTICLE INFO

Article history:
Received 11 July 2025
Received in revised form 15 August 2025
Accepted 6 January 2026

Keywords:
Antrodia camphorata
High-fat diet
Insoluble dietary fiber
Ruminococcaceae
Lipid metabolic disorders

ABSTRACT

High-fat diets (HFD) disrupt lipid homeostasis, posing major public health risks. This study investigated the effect of ACA-DK, an insoluble dietary fiber derived from *Antrodia camphorata*, on HFD-induced dyslipidemia. We demonstrate that ACA-DK effectively alleviates HFD-induced dyslipidemia in mice, counteracting metabolic disorders, aberrant blood lipids, and weight gain. Mechanistically, ACA-DK modulates triglycerides, phosphatidylcholine, and phosphatidylethanolamine *via* glycerophospholipid/choline/linoleic acid metabolism pathways, while rectifying gut dysbiosis through selective reduction of pro-inflammatory genera (*Oscillibacter*, *Ruminiclostridium*, *Negativibacillus*, Ruminococcaceae and *Helicobacter*). Integrated analysis identifies Ruminococcaceae and *Helicobacter* as key mediators of ACA-DK's lipid-regulatory effects, establishing microbiota-directed therapy as a strategy against dyslipidemia. We thus propose ACA-DK as a microbiota-directed dual-target therapy, simultaneously reprogramming host lipid metabolism and gut ecology to combat diet-induced metabolic diseases. These findings suggest that ACA-DK is a promising prebiotic dietary fiber for ameliorating HFD-induced lipid metabolic disorders, with potential for future development into functional foods or supplements.

1. Introduction

Long-term consumption of a high-energy, high-saturated fatty acid, and high-cholesterol diet can disrupt lipid synthesis, decomposition, transformation, and transportation, significantly increasing the risks of hyperlipidemia, cardiovascular disease, and type 2 diabetes[1-3]. The effects of high-fat diets (HFD) on metabolism are not only due to simple accumulation but also influenced by gender and critical developmental stages[4]. HFD have also been linked to an increased risk of cancer, especially cancers of the digestive system, such as colorectal cancer[5-6], and found to induce inflammation in tissues such as the intestine, destroy the intestinal barrier function, and disrupt the gut microbial rhythm[7-8]. Statins and phenoxy acids are commonly used to treat hyperlipidemia and have demonstrated good efficacy and rapid onset of action. However, long-term use of these drugs causes adverse effects, such as headache, dizziness, and rash, and requires strict dietary control[9].

Enhancing diet with dietary fiber is an effective strategy for mitigating the adverse effects of HFD[10]. Dietary fiber, a group of carbohydrates that cannot be absorbed by the small intestine but are fermented in the colon, has been shown to effectively control metabolic disorders such as lipid and blood glucose abnormalities[11-12]. The type

* Corresponding authors.
E-mail address: dreamup@126.com (Y.J. Xia); jessyshen72@sina.com (T.T. Shen)
Peer review under responsibility of Beijing Academy of Food Sciences.

SciOpen Publishing services by Tsinghua University Press

http://doi.org/10.26599/FSHW.2026.9250938

of dietary fiber considerably influences its effect on metabolic disorders. Soluble dietary fiber, such as oat β-glucan, undergoes extensive fermentation in the intestine, which can promote the production of short-chain fatty acids, decrease total cholesterol (TC) and low-density lipoprotein cholesterol (LDL-C) levels in the blood, and alleviate HFD-induced damage[13]. Conversely, insoluble dietary fiber, such as cellulose in whole grains, is less fermented in the intestine but enhances intestinal peristalsis and reduces fat absorption[14-15]. It also facilitates the fecal excretion of cholesterol, decreases its accumulation in the body, and indirectly improves lipid metabolism by improving insulin sensitivity, especially in individuals with obesity and diabetes[16]. However, the potential of novel insoluble dietary fibers to rectify these diet-induced perturbations remains underexplored.

The gut microbiota plays a pivotal role in addressing metabolic disorders. Yang et al.[17] demonstrated that HFD promote colorectal tumorigenesis by disrupting the balance of the gut microbiota and their metabolites. Additionally, gut microbiota changes caused by HFD may influence the host's appetite and energy intake, potentially causing excess energy intake and weight gain[18]. Gut microbiota imbalances also disrupt the liver-intestine circulation of bile acids, affecting hepatic lipid metabolism[19].

In contrast to well-studied fibers from grains and legumes, dietary fibers derived from edible fungi represent a promising but underexplored resource[20-21]. Previously, we successfully isolated an insoluble dietary fiber named ACA-DK from an *Antrodia camphorata* residue using the sodium hydroxide-dimethyl sulfoxide extraction technique. ACA-DK, appearing as irregular fragments, has shown strong *in vitro* absorption capabilities, especially for oil, cholesterol, and sodium cholate[22]. ACA-DK's low water solubility may limit its fermentation in the intestine. However, the role of ACA-DK in regulating lipid homeostasis *via* the gut-liver axis remains unexplored. This study investigated the hypolipidemic effects of ACA-DK using an integrated analysis of the gut microbiome and host metabolome. Our results reveal a novel mechanism centered on glycerophospholipid metabolism, which provides new strategies for preventing and treating metabolic diseases related to HFD.

2. Materials and methods

2.1 Materials and diet

A. camphorata residue was gifted by Honest and Humble Biotechnology Co., Ltd. (New Taipei City, China). Based on our previously published methodology[22], the production and purification of ACA-DK were summarized as follows: ACA-DK was alkali-extracted from the residue of *A. camphorata* (after hot-water and ethanol extraction) using a 0.5 mol/L NaOH/0.01 mol/L $NaBH_4$ solution at 4 °C for 12 h. The extract was then neutralized, treated with a DMSO/LiCl solution, dialyzed, and freeze-dried to obtain the final insoluble dietary fiber. The purity of the extracted ACA-DK was determined by using a HPLC system (Waters 1525 system, Agilent PLgel MIXED column, 300 mm × 7.5 mm, 5 μm), with DMSO as the mobile phase at a flow rate of 1 mL/min at 35 °C.

2.1.2 Diet of Animal experiment

The animal experiments used a basic diet comprising 20% flour, 25% bran, 20% corn, 10% rice flour, 20% legumes, 2% fish meal, 2% bone meal, 0.9% salt, and 0.1% vitamins and an HFD comprising 10% lard, 5% sucrose, 1% cholesterol, 0.3% bile salt, and 83.7% basic feed. Both types of feed were ordered from Nantong Trophe Feed Technology Co., Ltd. (Nantong, China).

2.2 Polysaccharides analysis

Specific pathogen-free C57BL/6 male mice (5–6 weeks old, 20–22 g) were purchased from Shanghai JieSiJie Laboratory Animal Co., Ltd. (Shanghai, China) and housed in individually ventilated cages (BCR-MI03, Shinva Medical Instrument Co., Ltd., Shandong, China) maintained at (22 ± 2) °C temperature and 50% humidity. Before the experiment, the mice were adaptively fed for a week with free access to water and basic feed. After the end of the adaptation period, the mice were randomly divided into 4 groups, with no significant weight differences among them: normal control (Con), HFD/model (Mod), low-dose ACA-DK (Cur1, 200 g/kg), and high-dose ACA-DK (Cur2, 500 g/kg). Each group contained 10 mice, which were fed with the basic feed or the high-fat feed. The grouping scheme is shown in Table 1. The experiment was conducted for 8 consecutive weeks, during which the mice had free access to food and water and their body weight was measured weekly. All experiments were approved and performed following the animal protocol guidelines of the Institutional Animal Care and Use Committee of Shanghai Shi Dong Hospital (2023-031-01).

Table 1
Animal experiment grouping scheme.

No.	Group	Feed	Oral gavage
1	Con	Basic feed	Saline solution
2	Mod	HFD	Saline solution
3	Cur1	HFD	200 mg/kg ACA-DK
4	Cur2	HFD	500 mg/kg ACA-DK

2.3 Fecal sample collection

On the last day of the experiment, mouse fecal samples were collected and stored in a −80 °C freezer for gut microbiome analysis.

2.4 Liver and serum sample preparation

After the final gavage, blood was collected by eyeball puncture 16–18 h later. The blood samples were centrifuged at 3 000 r/min for 10 min at 4 °C, and the supernatants containing the sera were stored at −80 °C for biochemical analysis. The livers were photographed to document their morphology and divided into portions for hematoxylin and eosin (HE) staining, Oil red O (ORO) staining, and biochemical analysis.

2.5 Biochemical index determination

Biochemical indicators of liver tissue and serum (TC, TG, LDL-C, high-density lipoprotein cholesterol (HDL-C), and malondialdehyde (MDA)) were measured using kits following the

manufacturer's instructions (Nanjing Jiancheng Bioengineering Institute, Nanjing, China). The activities of lipid metabolism-related enzymes (3-hydroxy-3-methylglutaryl coenzyme A (HMG-CoA), diacylglycerol acyltransferase (DGAT), fatty acid synthase (FAS), fatty acid *β*-oxidation (FaβO), hepatic lipase (HL)) in the liver were analyzed using enzyme-linked immunosorbent assay kits following the manufacturer's instructions (Shanghai Tongwei Biotechnology Co., Ltd., Shanghai, China).

2.6 Pathological staining

The morphological analysis of mouse livers was conducted using HE and ORO staining. Liver tissue was fixed in 10% neutral formalin for 18 h, dehydrated, and then embedded in paraffin to prepare sections (4 μm) for HE staining or in optimal cutting temperature compound to prepare sections (10 μm) for ORO staining.

2.7 Liver lipid metabolome analysis

A total of 50 mg liver tissue was added to a 1.5-mL centrifuge tube and homogenized with 800 μL of extraction solvent (methanol:water = 1:1). Thereafter, 800 μL of chloroform was added and extraction was performed with low-temperature ultrasonication for 30 min (5 °C, 40 kHz). The sample was left undisturbed at −20 °C for 30 min and then centrifuged for 15 min (13 000 × *g*, 4 °C). The supernatant (350 μL) was transferred into an Eppendorf tube, dried under nitrogen flow, and reconstituted with 100 μL of extraction solvent (isopropanol:acetonitrile = 1:1). This was followed by vortexing for 30 s, extraction with low-temperature ultrasonication for 5 min (5 °C, 40 kHz), and centrifugation for 10 min (13 000 × *g*, 4 °C). The supernatant was separated for LC-MS/MS analysis.

LC-MS/MS conditions: the UHPLC-Q Exactive HF-X system (Thermo Fisher Scientific) was used with an Accucore C_{30} column (100 mm × 2.1 mm, 2.6 μm; Thermo). Mobile phase A was a 50% aqueous acetonitrile solution containing 0.1% formic acid and 10 mmol/L ammonium acetate. Mobile phase B was a mixture of acetonitrile/isopropanol (10:90) containing 0.1% formic acid and 10 mmol/L ammonium acetate. The injection volume was 5 μL, and the column temperature was set at 45 °C. Separation gradient: 0−4 min, 5% mobile phase B; 4−25 min, 5%−95% mobile phase B; 25−30 min, mobile phase B maintained at 95%. The flow rate was 0.40 mL/min.

Mass spectrometry conditions: the mass spectrometry signal acquisition for the samples was conducted using both positive and negative ion scanning modes, with a mass scanning range (*m*/*z*) from 135 to 2 000. The spray voltage was set at 3 000 V for positive ions and at 2 500 V for negative ions. The declustering potential was 80 V, the nebulizer gas pressure was 60 psi, and the auxiliary heating gas pressure was 20 psi. The ion source heating temperature and capillary temperature were maintained at 300 and 350 °C, respectively.

2.8 16S rRNA gene sequencing of the gut microbiota

The total microbial genomic DNA was extracted using the E.Z.N.A.® soil DNA kit (Omega Bio-tek, Norcross, GA, USA) following the manufacturer's instructions. The DNA concentration and quality were measured using NanoDrop 2000 (Thermo Scientific, USA). The universal primers 338F (5′-ACTCCTACGGGAGGCAGCAG-3′) and 806R (5′-GGACTACHVGGGTWTCTAAT-3′) were used to amplify the V3–V4 variable region of the 16S rRNA gene using PCR. The PCR program was as follows: initial denaturation at 95 °C for 3 min, followed by 27 cycles of denaturation at 95 °C for 30 s, annealing at 55 °C for 30 s, and extension at 72 °C for 30 s, then a final extension at 72 °C for 10 min, and final storage at 4 °C (PCR instrument: ABI GeneAmp® 9700). The PCR reaction mixture comprised 4 μL 5× Fast Pfu buffer, 2 μL 2.5 mmol/L dNTPs, 0.8 μL each primer (5 μmol/L), 0.4 μL Fast Pfu DNA polymerase, 10 ng of template DNA, and made up to 20 μL with ddH_2O. All samples were amplified in triplicate. The PCR products were recovered using a 2% agarose gel and purified using the AxyPrep DNA Gel Extraction kit (Axygen Biosciences, Union City, CA, USA). The purified products were quantified using the Quantus™ Fluorometer (Promega, USA) and sequenced on an Illumina MiSeq platform (Illumina, USA) at Majorbio Bio-Pharm Technology Co., Ltd., Shanghai, China.

2.9 Microbiota analysis

Microbial analysis of the samples was performed using Majorbio Cloud (https://cloud.majorbio.com; Majorbio Bio-Pharm Technology Co., Ltd., Shanghai, China). The raw reads were quality-controlled using fastp (version 0.19.6). FLASH (version 1.2.11) was used for reading assembly. The optimized sequences after quality control and assembly were subjected to denoising using the DADA2 plugin within the QIIME2 pipeline. All sample sequences were rarefied to 20 000 reads, after which the average sequence coverage (Good's coverage) of each sample still reached 99.09%. Based on the Silva 16S rRNA gene database (version 138), the species-level taxonomic analysis of amplicon sequence variants (ASVs) was conducted using the Naive Bayes classifier within QIIME2. The functional prediction analysis of the 16S rRNA was performed using PICRUSt2 (version 2.2.0).

2.10 Data analysis

Bioinformatic analysis of the gut microbiota was performed using Majorbio Cloud (https://cloud.majorbio.com). The *α*-diversity analysis was conducted using Welch's *t*-test. The similarity of the microbial communities between different samples was assessed using principal coordinate analysis (PCoA) based on Bray-Curtis dissimilarity using the Vegan v2.5-3 package. Statistical analysis of physical and chemical indexes of urine was performed using ANOVA in SPSS 24.0. P value < 0.05 was considered statistically significant.

3. Results

3.1 ACA-DK improves HFD-induced dyslipidemia

We administered two dosages of ACA-DK (200 and 500 mg/kg) *via* gavage to HFD-fed mice to assess their effects on body weight and serum lipid profiles (Fig. 1A). The results revealed that ACA-DK supplementation notably curbed weight gain in these mice compared with the model mice. The Cur2 group (500 mg/kg) exhibited a marked reduction in body weight compared with both the Mod and Cur1 (200 mg/kg) groups, with no significant difference in weight relative to the Con group (Fig. 1B).

In terms of lipid metabolism, the Cur2 group showed greater improvements in lipid abnormalities in both the serum and liver than the Cur1 group. ACA-DK supplementation significantly reduced TC, TG, and LDL-C levels while increasing HDL-C levels (Figs. 1C and D). The organ indices of the liver, kidneys, and spleen, to a certain extent, reflect the degree of liver damage and the body's physiological condition. The kidney index was similar in the Mod and Con groups ($P > 0.05$), whereas liver and spleen indices were significantly elevated in the former ($P < 0.05$) (Table 2). ACA-DK supplementation markedly reduced the liver and spleen indices, with no discernible difference between the Cur1 and Cur2 groups.

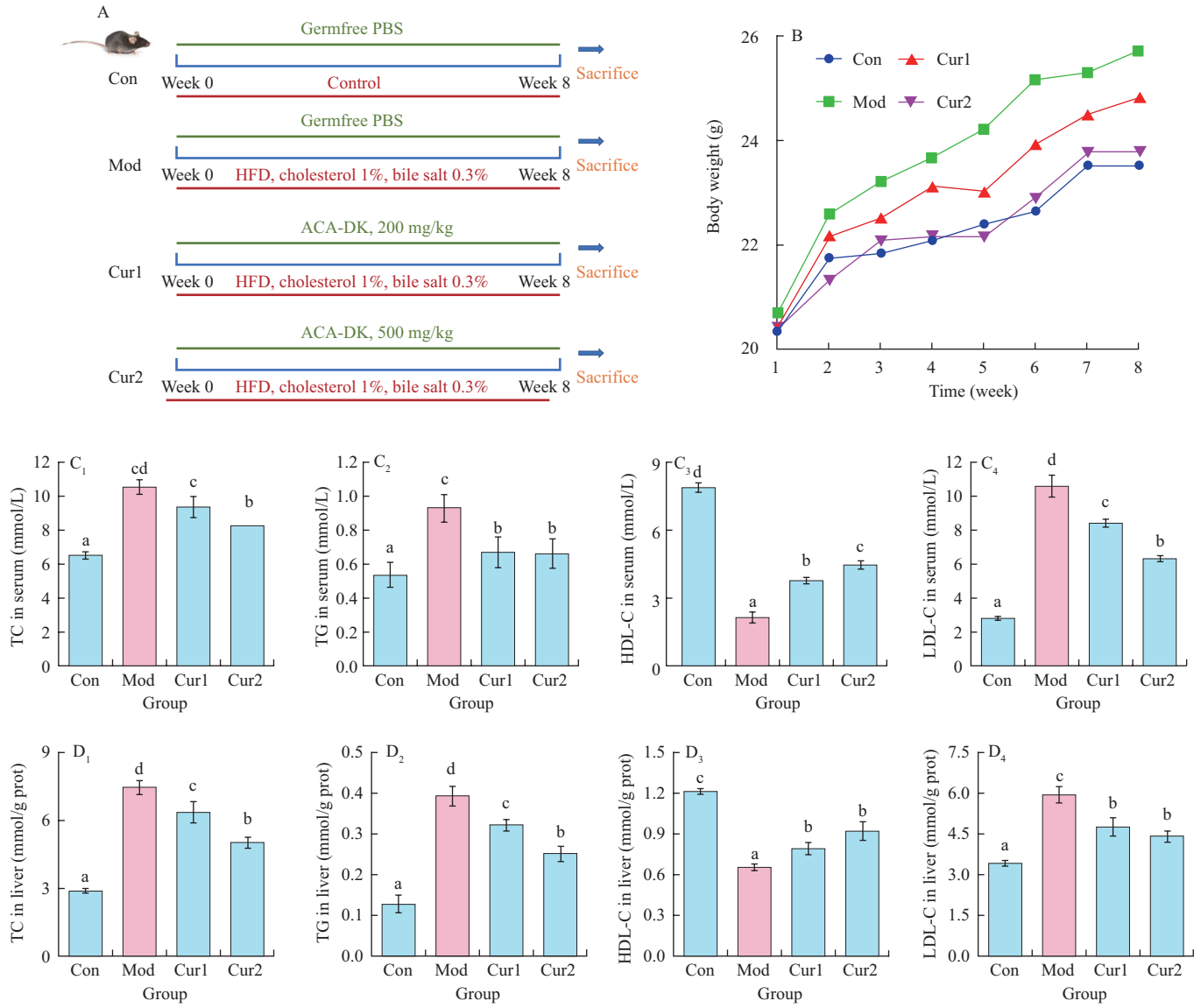

Fig. 2 Impact of ACA-DK on the body weight and lipid metabolic indicators of mice on an HFD. (A) Experimental flowchart; (B) Changes in body weight; (C) Lipid metabolic indicators in mouse serum; (D) Lipid metabolic indicators in mouse liver. Data were presented as means ± SD. One-way ANOVA with Duncan's post hoc test, different letters mean significantly different ($P < 0.05$).

Table 2
Organ indices of mice in different groups.

Organs	Con	Mod	Cur1	Cur2
Liver	3.42 ± 0.08^{a}	4.63 ± 0.11^{c}	4.51 ± 0.09^{b}	4.34 ± 0.05^{b}
Spleen	0.28 ± 0.07^{a}	0.47 ± 0.10^{c}	0.37 ± 0.07^{b}	0.36 ± 0.03^{b}
Kidney	1.08 ± 0.03^{a}	1.10 ± 0.02^{a}	1.00 ± 0.06^{a}	1.07 ± 0.04^{a}

Note: Different letters indicate statistically significant differences based on ANOVA ($P < 0.05$).

3.2 ACA-DK effectively regulates the liver's lipid metabolic capacity

Liver tissue morphology can illustrate the effects of an HFD on mouse livers. As shown in Fig. 2A, the livers of HFD mice (Mod group) appeared pale, dull, and lacked luster. This pathological phenotype was ameliorated in a dose-dependent manner by ACA-DK, with the Cur2 group showing the most notable improvement in color and size, which was corroborated by a significant reduction in liver index (Table 2). Histological evaluation using HE staining demonstrated that ACA-DK significantly attenuated the HFD-induced inflammatory infiltration in the liver. The hepatocytes were arranged in a regular pattern with clear and intact nuclei, and the degree of vacuolar degeneration was significantly reduced (Fig. 2B). The ORO staining results confirmed that ACA-DK decreased fat accumulation in the liver, particularly in the Cur2 group (Fig. 2C). Further, the MDA content in the livers of HFD-fed mice was significantly increased compared with basic diet-fed mice, indicating the presence of lipid oxidative damage. After ACA-DK administration, the MDA content significantly decreased, especially in the Cur2 group (Fig. 2D).

HFD significantly affects the hepatic lipid metabolic capacity. Therefore, we measured lipid metabolism-related enzymes in the liver of mice. Our findings demonstrated that the HFD significantly reduced the activities of FaβO and HL, whereas ACA-DK supplementation markedly enhanced their activities in the liver tissue, with no significant difference between the Cur1 and Cur2 groups (Figs. 2E and F). Figs. 2G and H demonstrate the effect of ACA-DK on enzymes associated with lipid synthesis pathways in the liver. The Mod group showed a significant increase in the activities of enzymes, particularly HMG-CoA, DGAT, and FAS, involved in lipid synthesis compared with the Con group. Among these enzymes, HMG-CoA and DGAT showed the highest activity increases of 55.5% and 98.6%, respectively, compared with the Con group.

ACA-DK supplementation significantly reduced the activities of these enzymes, with high-dose ACA-DK exerting a more pronounced effect than low-dose on HMG-CoA and DGAT activities.

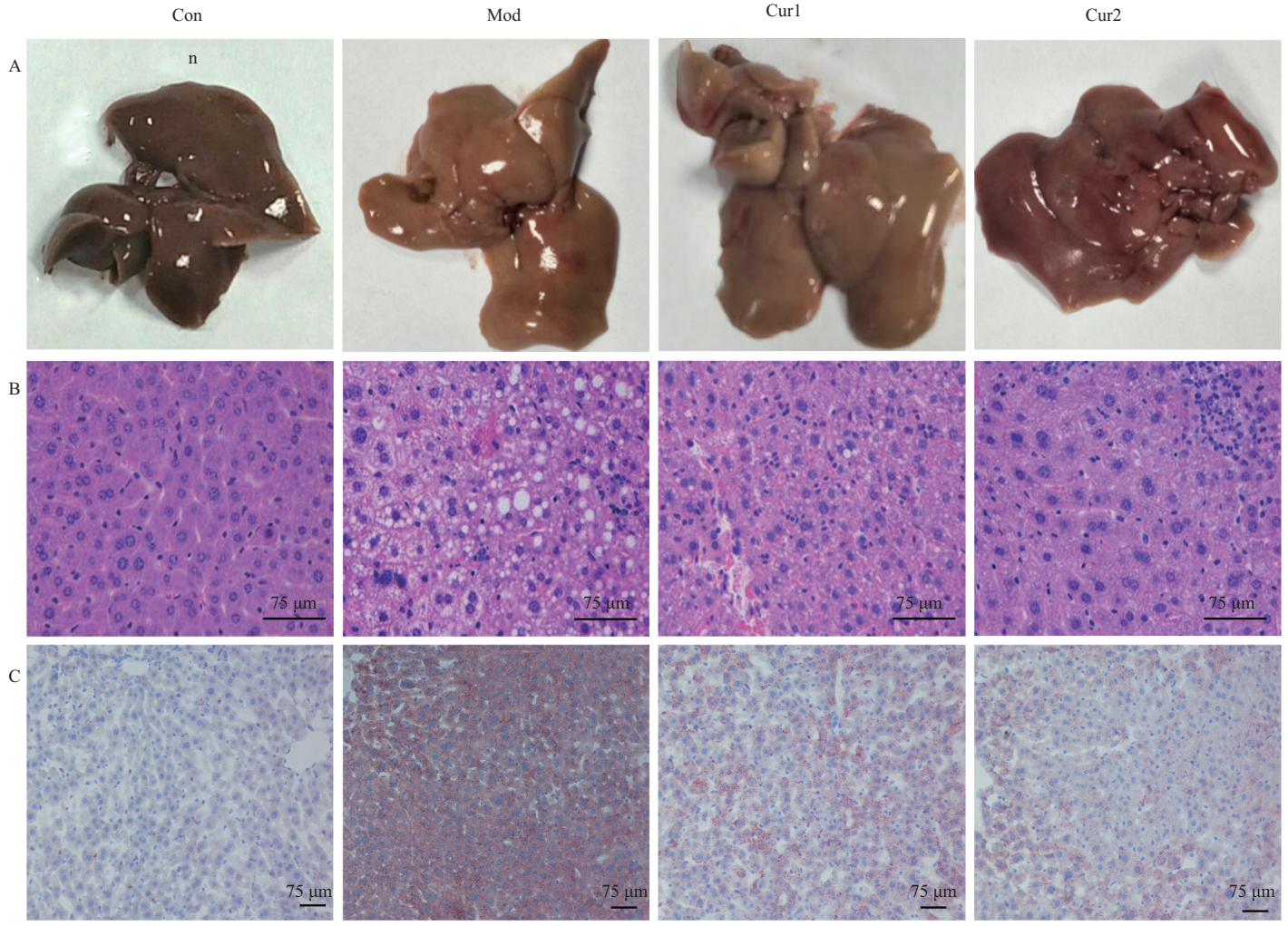

Fig. 2 Impact of ACA-DK on liver morphology and lipid metabolism capabilities. (A) Liver morphology; (B) HE staining analysis; (C) ORO staining analysis; (D) Liver MDA content; (E) Liver FA enzyme activity; (F) Liver HL enzyme activity; (G) Liver HMG-CoA enzyme activity; (H) Liver DGAT enzyme activity; (I) Liver FAS enzyme activity. Data were presented as means ± SD. One-way ANOVA with Duncan's post hoc test, different letters mean significantly different ($P < 0.05$). Scale bar = 75 μm.

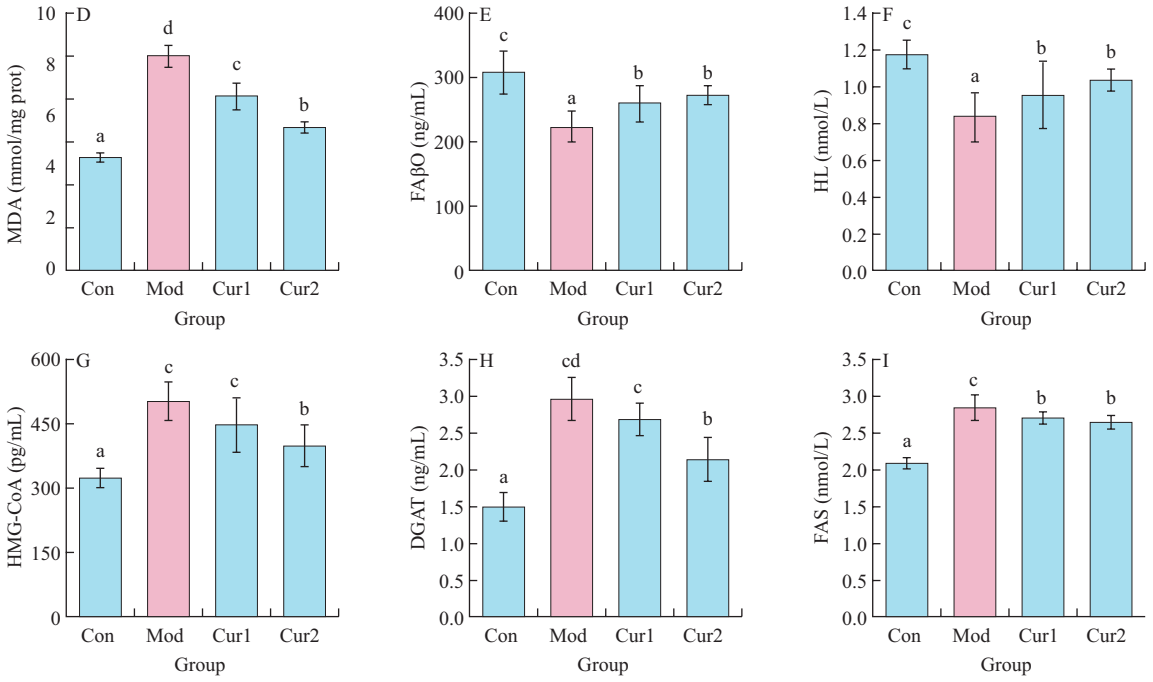

Fig. 2 (*Continued*)

3.3 ACA-DK significantly affects the hepatic lipid composition

Research indicates that high-dose ACA-DK is more effective than low-dose ACA-DK in mitigating HFD-induced disruptions in lipid metabolism. Consequently, we used lipid metabolic profiling to analyze the hepatic lipid composition in mice. Overall, 2 441 lipid compounds were detected under both positive and negative modes, which were classified into 25 classes such as triglycerides (TG), phosphatidylcholine (PC), phosphatidylethanolamine (PE), phosphatidylglycerol (PG), and ceramide.

We established 2 sets of differential metabolites using metabolite analysis: Con *vs*. Mod and Cur2 *vs*. Mod ($P < 0.05$, variable importance in projection (VIP) > 1, fold change > 1.2). The orthogonal partial least squares-discriminant analysis (OPLS-DA) analysis revealed significant differences in metabolites between the Con and Mod groups and between the Cur2 and Mod groups (Figs. 3A and B). Lipid metabolites were significantly upregulated in the Mod group, with the top 6 upregulated metabolites being TG (186), PC (120), PE (84), cardiolipin (CL) (77), diacylglycerol (DG) (59), and PG (41) (Fig. 3C). Conversely, lipid metabolites were markedly downregulated in the Cur2 group, with the top 7 downregulated metabolites being TG (33), PE (10), DG (7), PI (5), PS (5), PC (5) and Cer (5) (Fig. 3D).

Figs. 3E and F provide a comparative assessment of lipid metabolite levels. Compared with the Con group, lipid metabolite levels were increased in the Mod group, including a notable upregulation of phosphatidylinositol (PI), PG, phosphatidylserine (PS), PC, PE, and choline esterase (ChE) metabolites. Conversely, the Cur2 group exhibited a significant decline in the levels of these lipid metabolites, notably PC, PE, and PG. From the comparative lipidomic sets of Con *vs*. Mod and Cur2 *vs*. Mod, the 50 most significantly altered lipid metabolites, as determined by their VIP scores, were selected for subsequent cluster analysis. This analysis demonstrated that high-dose ACA-DK supplementation significantly ameliorated the lipid metabolism dysregulation typically associated with HFD (Fig. S1).

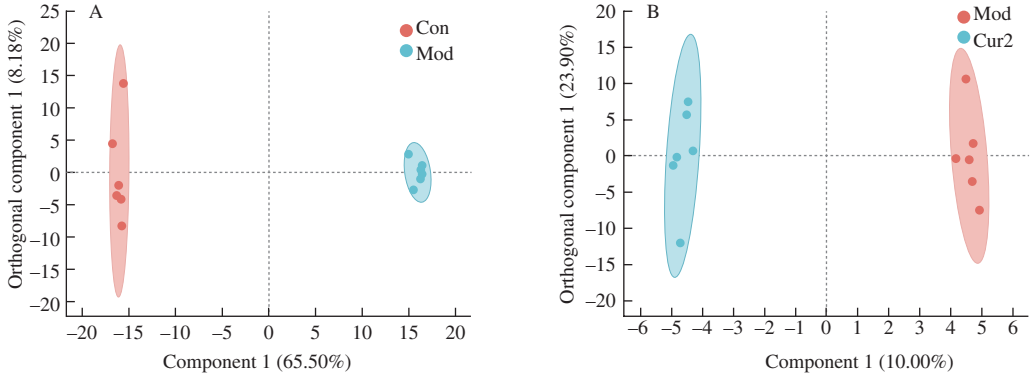

Fig. 3 Impact of ACA-DK on the liver lipid composition of mice fed an HFD. (A) OPLS-DA analysis of lipids in the metabolic profile of Con *vs.* Mod; (B) OPLS-DA analysis of lipids in the metabolic profile of Cur2 *vs.* Mod; (C) Species distribution of lipid compounds in the metabolic profile of Con *vs.* Mod; (D) Species distribution of lipid compounds in the metabolic profile of Cur2 *vs*. Mod; (E) Content distribution of lipid compounds in the metabolic profile of Con *vs.* Mod; (F) Content distribution of lipid compounds in the metabolic profile of Cur2 *vs.* Mod.

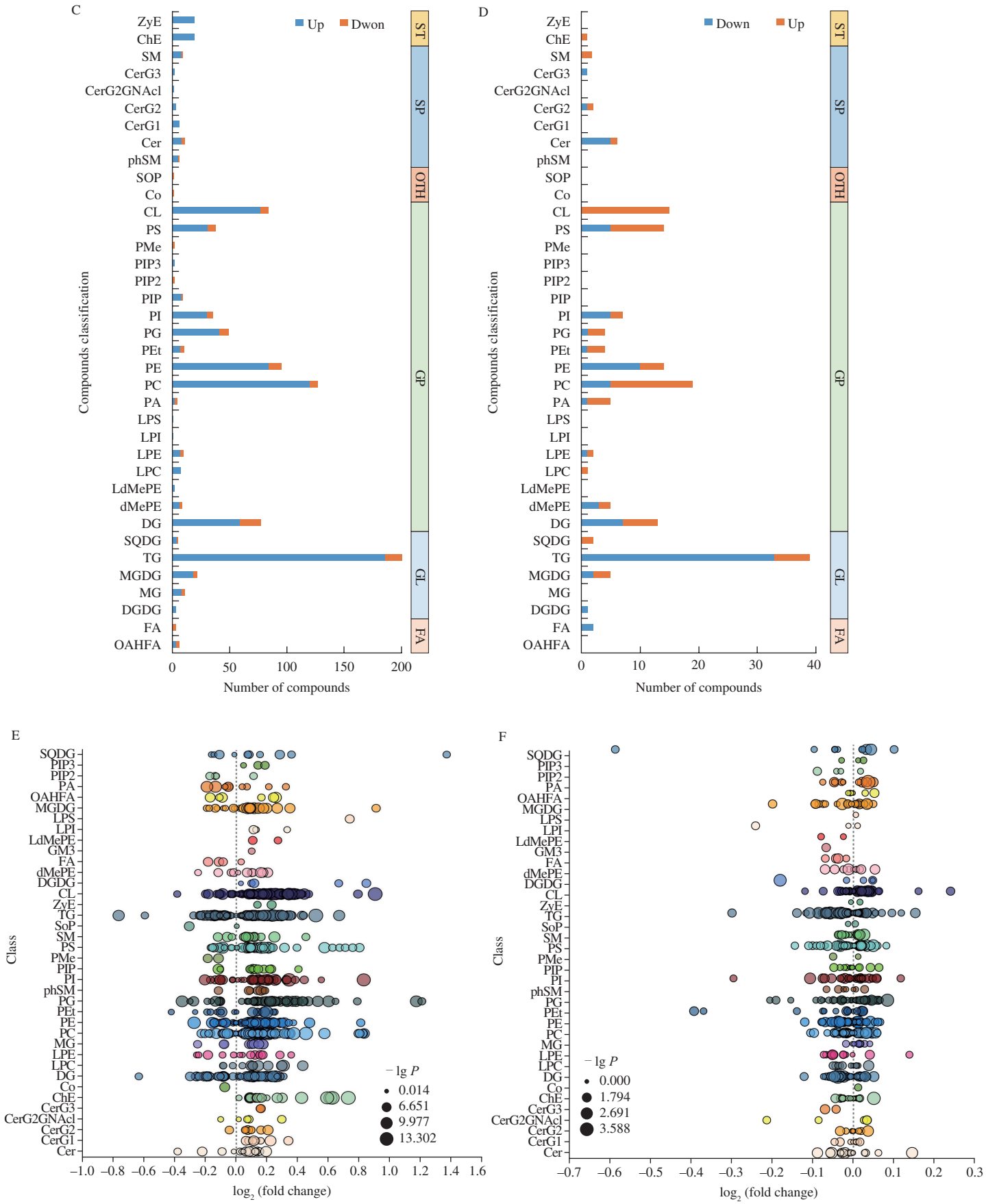

Fig. 3 (*Continued*)

3.4 Analysis of differential lipid metabolites

To further examine the effects of various lipid metabolites, we analyzed the relationships between the top 60 lipid metabolites, as per their VIP rankings, and key hepatic lipid biomarkers, including TC and TG. As shown in Fig. 4A, in the HFD group, increases in TC and TG levels were significantly correlated with increases in TG, PS, and CL metabolites and certain PC and PG metabolites. Additionally, the rise in LDL-C levels was significantly correlated with increases in levels of long-chain TG, PS, ChE, and specific PC and PG metabolites. Correspondingly, the decline in HDL-C levels was significantly linked to alterations in lipid metabolites, including TG, PS, and PC.

Following high-dose ACA-DK administration, a pronounced correlation was observed between the hepatic levels of differential lipids, including PC and PS, and decreased TC, TG, and LDL-C levels. Notably, after ACA-DK administration, the TG profile changed significantly, with increases in medium- and long-chain TG exhibiting associations with TC, TG, and LDL-C levels (Fig. 4B). Furthermore, lipid metabolite analysis with respect to double bond counts revealed that ACA-DK administration markedly decreased the concentrations of metabolites with low double bond count, particularly within the lipid classes TG, PC, PE, and DG (Fig. S2). KEGG enrichment analysis of the differential lipid metabolites revealed a significant upregulation of pathways associated with lipid metabolism, nervous system, and cancer following an HFD, but enrichment of pathways related to glycerophospholipid metabolism, choline metabolism in cancer, and linoleic acid metabolism following ACA-DK treatment (Figs. 4C and D).

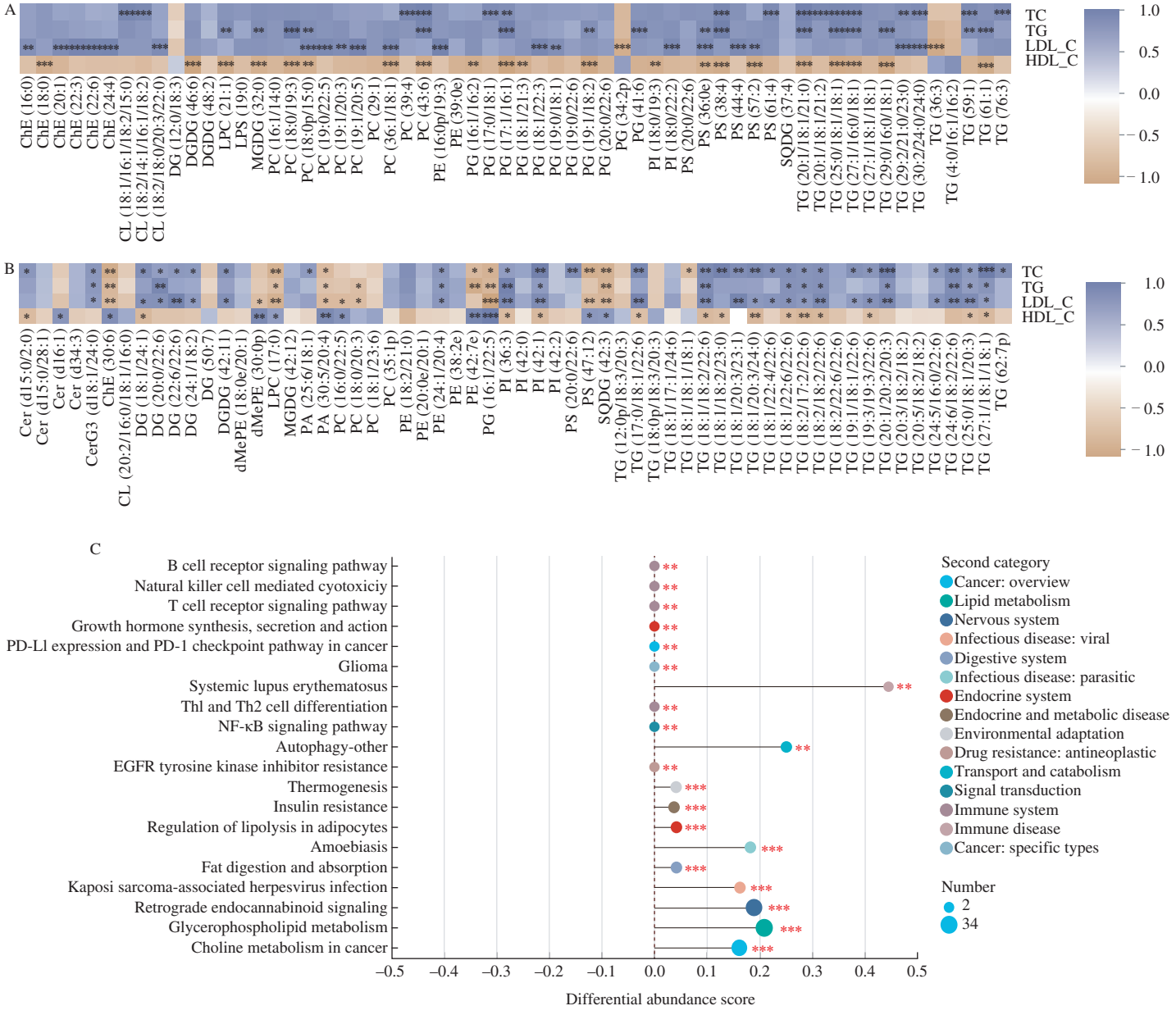

Fig. 4 Analysis of differential lipid metabolites. (A) Spearman correlation analysis between differential lipid metabolites and blood lipid parameters in the set of Mon *vs*. Con; (B) Spearman correlation analysis between differential lipid metabolites and blood lipid parameters in the set of Cur2 *vs*. Mod; (C) Metabolic pathway enrichment analysis of differential lipid metabolites in the set of Mon *vs*. Con; (D) Metabolic pathway enrichment analysis of differential lipid metabolites in the set of Cur2 *vs*. Mod. Significant differences were compared with each 2 groups, $^{*}P < 0.05$, $^{**}P < 0.01$, $^{***}P < 0.001$.

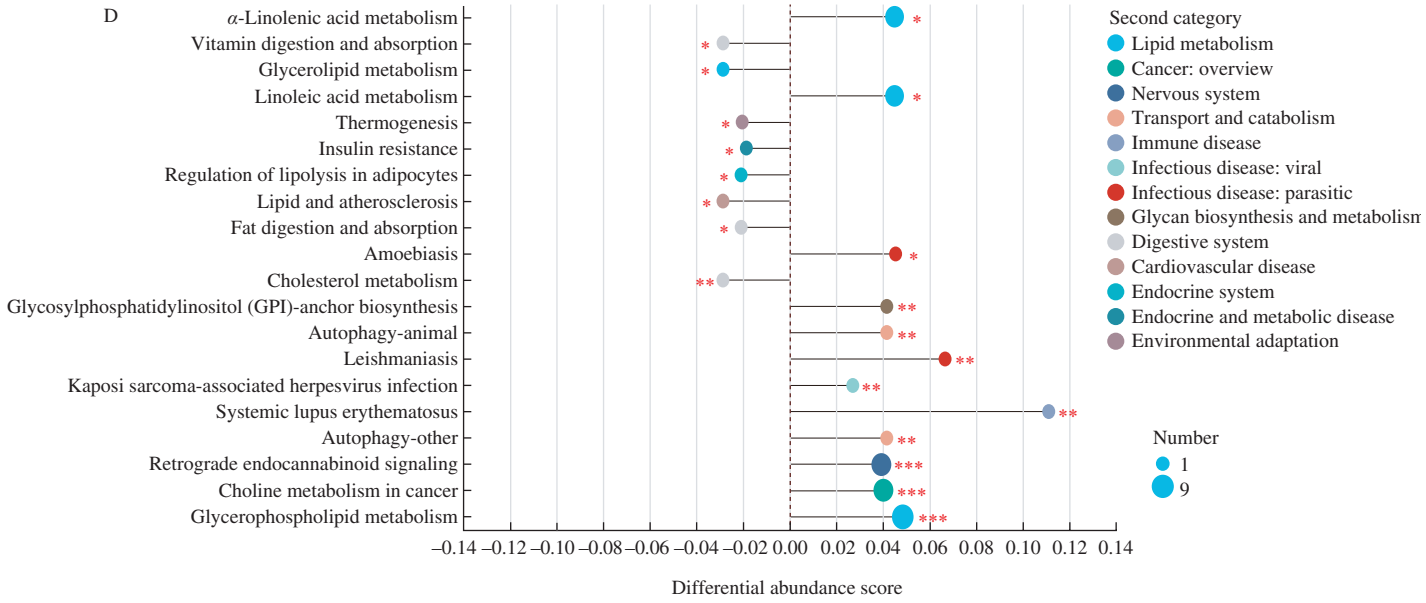

Fig. 4 (*Continued*)

3.5 ACA-DK alleviates the gut microbiota disorder caused by a HFD

High-throughput sequencing was used to assess the effect of ACA-DK on the gut microbiota (Fig. 5). Our findings demonstrated that the HFD significantly altered the gut microbiota at both the phylum and genus levels. ACA-DK supplementation ameliorated these diet-induced alterations, notably by reducing the abundance of Epsilonbacteraeota (Fig. 5A), but exerted no significant effect on the α-diversity of the gut microbiota (Fig. 5B). The PCoA results revealed clear divergence in the gut microbiota composition between the Mod and Con groups, with substantial shifts observed after the ACA-DK intervention (Fig. 5C). Despite its efficacy in ameliorating hyperlipidemia, the ACA-DK intervention led to a higher Firmicutes-to-Bacteroidota (F/B) ratio. Detailed analysis at the genus level revealed that this paradoxical increase was primarily driven by a bloom of specific, beneficial Firmicutes, particularly members of the Ruminococcaceae and Lachnospiraceae families, which are renowned for their ability to ferment dietary fiber and produce health-promoting short-chain fatty acids. Thus, the elevated F/B ratio reflects a therapeutic shift towards a fiber-degrading microbiome ecology.

Our examination of the gut microbiota imbalance index in mice revealed that the HFD markedly disrupted the gut microbiota equilibrium. However, ACA-DK supplementation significantly mitigated this imbalance (Fig. 5D). Fig. 5E illustrates the intergroup differences in the dominant gut microbial genera. Our analysis revealed that the core distinction conferred by ACA-DK was the significant and selective suppression of specific pro-lipogenic genera in the Cur2 group compared to the Mod group. Specifically, ACA-DK intervention significantly reduced the relative abundance of *Helicobacter* and several genera from the Ruminococcaceae family, notably Ruminococcaceae_UCG-009, *Ruminiclostridium*, and *Negativibacillus*. Furthermore, the gut microbiota phenotype was predicted and analyzed using Bugbase. Compared with the Con group, the gut microbiota phenotypes Stress_Tolerant, Anaerobic, and Forms_Biofilms were markedly diminished, whereas the phenotypes Contains_Mobile_Elements and Aerobic were significantly increased, in the Mod group (Fig. S3A). After ACA-DK supplementation, the changes in the gut microbiota phenotypes were reversed, especially the phenotypes of anaerobic and aerobic. Further analysis revealed that the increase in aerobic phenotypes in the Mod group was mainly due to the increased abundance of *Helicobacter* (Fig. S3B).

3.6 The core gut microbes regulated by ACA-DK in lipid metabolism regulation

We performed a Spearman correlation analysis of the top 50 gut microbes related to blood lipid profiles, including TC, TG, LDL-C, and HDL-C, regulated by ACA-DK to identify the core gut microbes. The results showed that the genera *Lactobacillus*, *Faecalibaculum*, Muribaculaceae, *Bifidobacterium*, and Ruminococcaceae_UCG-014 were significantly negatively correlated with TC, TG, and LDL-C levels but significantly positively associated with HDL-C levels (Fig. 6A). Conversely, the genera *Helicobacter*, Ruminococcaceae_UCG-009, *Ruminiclostridium*, *Negativibacillus*, and *Oscillibacter* were positively correlated with TC, TG, and LDL-C levels but negatively correlated with HDL-C levels.

Compared with the Con group, the relative abundances of certain microbial genera, namely *Helicobacter*, Ruminococcaceae_UCG-009, *Ruminiclostridium*, *Negativibacillus* and *Oscillibacter*, were markedly elevated in the HFD group. This trend was reversed following ACA-DK administration, indicated by a significant reduction in the relative abundances of these genera in the Cur2 group (Fig. 6B). Our Spearman correlation analysis confirmed that these specific genera were positively correlated with serum TC, TG, and LDL-C levels (Fig. 6A), identifying them as potential promoters of HFD-induced dyslipidemia. Furthermore, the HFD decreased the abundance of beneficial genera such as *Lactobacillus* and *Bifidobacterium* (Fig. 5E). Although ACA-DK supplementation increased their relative abundances, the difference was not significant compared with the Mod group (Fig. 6B). This indicates that the modulation of the gut microbiota by ACA-DK is highly selective, and its lipid-

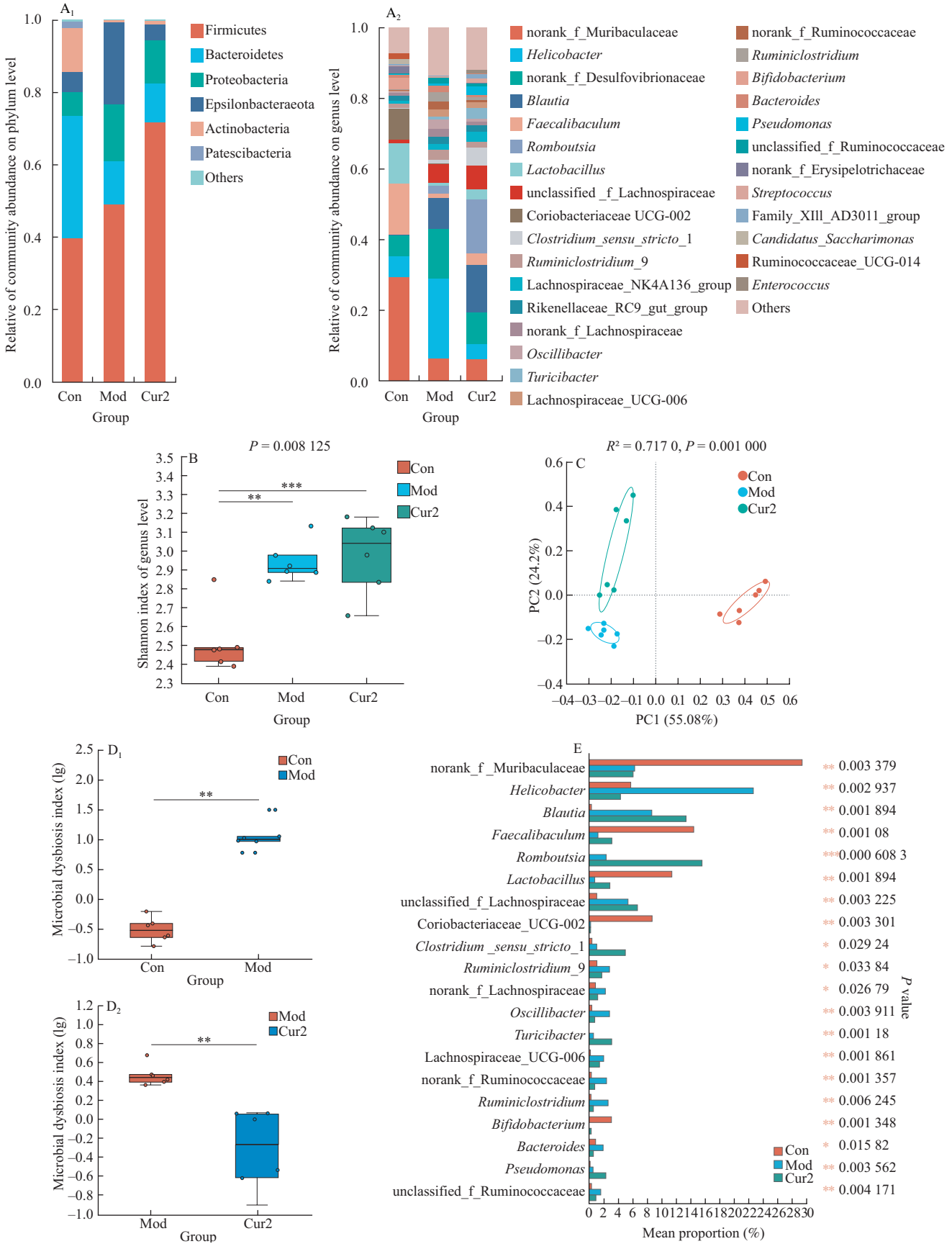

Fig. 5 Impact of ACA-DK on the gut microbiota of HFD mice. (A) Community analysis of the gut microbiota on phylum and genus levels; (B) *α*-Diversity changes of gut microbiota; (C) PCoA analysis of gut microbiota; (D) The imbalance index analysis of gut microbiota; (E) Phylotypes significantly different between Con, Mod and Cur2 group on genus level. Significant differences were compared with each 2 groups, $*P < 0.05$, $**P < 0.01$, $***P < 0.001$.

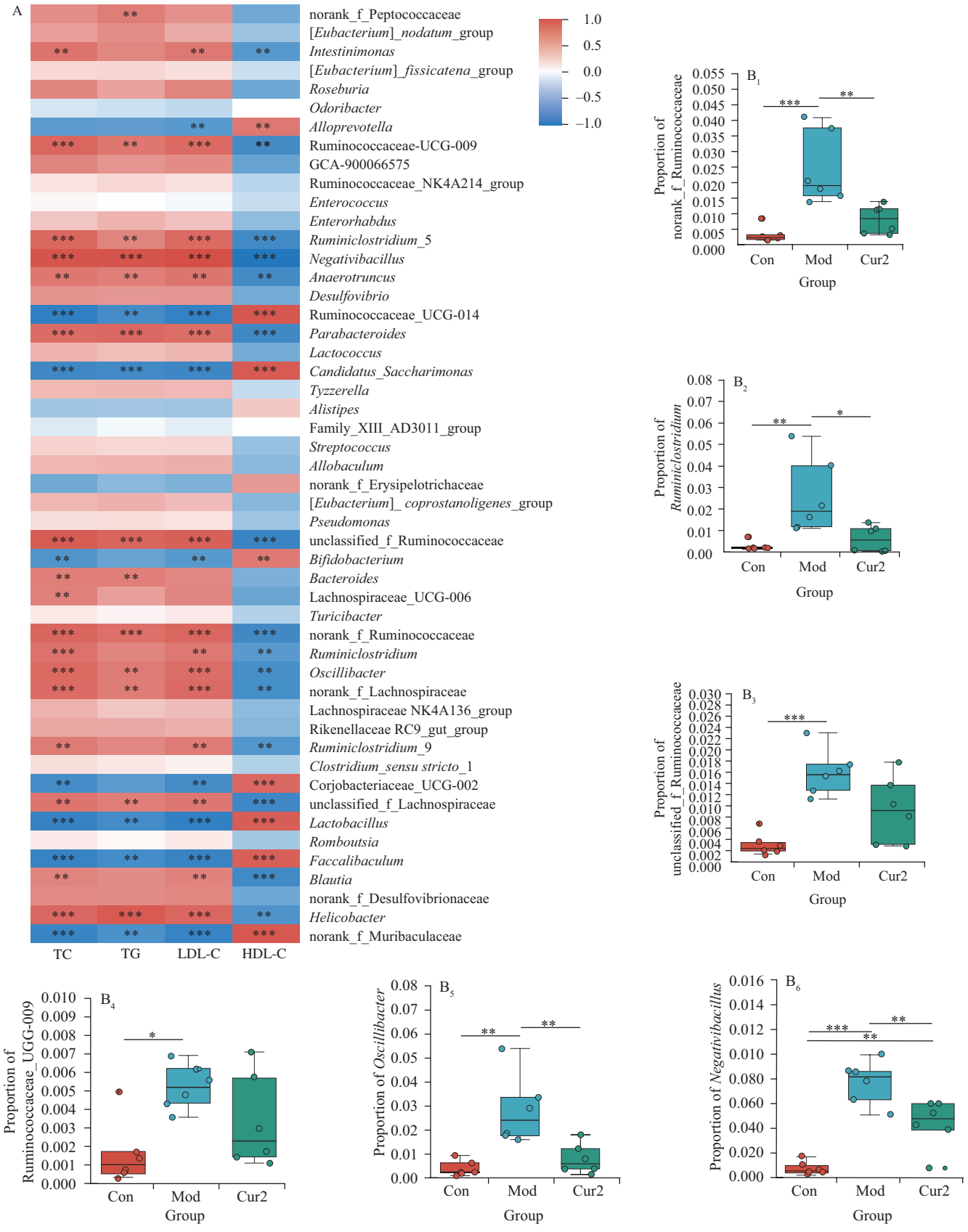

Fig. 6 Screening for core gut microbiota regulated by ACA-DK in lipid metabolism. (A) Spearman correlation analysis of gut microbes and blood lipid measures; (B) Comparative analysis of the relative content of gut microbiota; (C) Comparative analysis of the relative content of Ruminococcaceae family; (D) MaAslin analysis of gut microbes and TC. Significant differences were compared with each 2 groups, $*P < 0.05$, $**P < 0.01$, $***P < 0.001$.

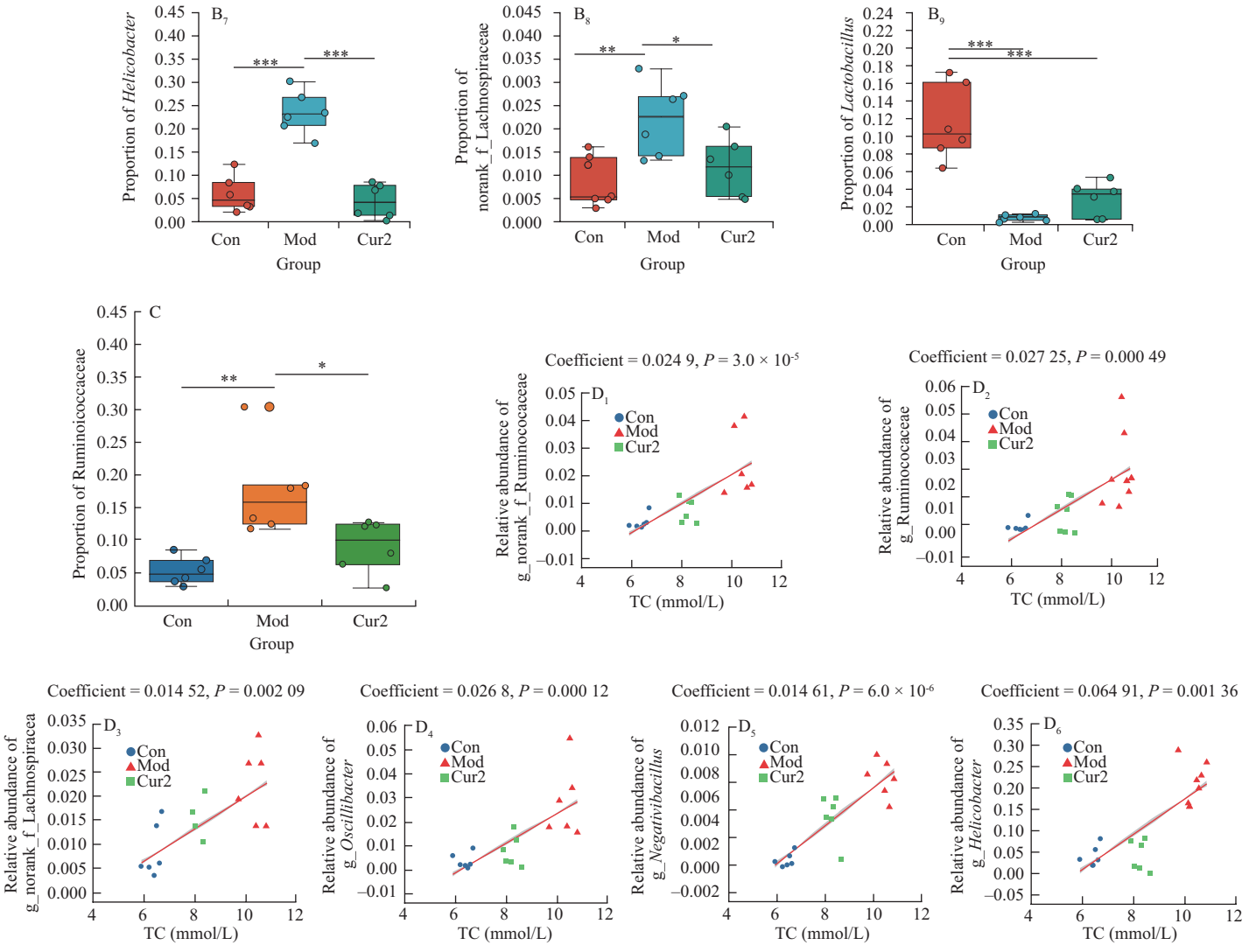

Fig. 6 (*Continued*)

improving effects are likely mediated primarily through the targeted suppression of specific harmful bacterial consortia rather than a broad promotion of all beneficial bacteria. Taxonomic analysis of the differentially abundant genera revealed that Ruminococcaceae_UCG-009, *Ruminiclostridium*, *Negativibacillus*, and *Oscillibacter* are members of the Ruminococcaceae family. Thereafter, we performed a comparative analysis of the 50 most abundant microbial families, demonstrating that ACA-DK treatment effectively counteracted the HFD-induced proliferation of the Ruminococcaceae family (Fig. 6C). We performed MaAslin analysis to substantiate the link between the core gut microbes and TC levels (Fig. 6D). The results confirmed that the pronounced elevation in the abundances of *Helicobacter*, Ruminococcaceae_UCG-009, *Ruminiclostridium*, *Negativibacillus*, and *Oscillibacter* was correlated with elevated TC levels.

3.7 Correlation analysis between the metabolome and gut microbiota

We analyzed the correlation between the top 60 differential lipid metabolites ranked by VIP and the top 50 differential microbes ranked by relative abundance under HFD conditions. The abundances of the genera *Helicobacter*, *Oscillibacter*, *Ruminiclostridium*, *Negativibacillus*, and *Intestinimonas* were positively associated with TG, PI, and DG metabolites but negatively associated with PA, PC, and PE metabolites (Fig. 7). These genera can significantly affect blood lipid metabolism levels, which is consistent with the results of previous studies (Fig. 4). Conversely, the correlation analysis of other genera, namely *Faecalibaculum*, *Romboutsia*, and *Leuconostoc*, revealed an inverse relationship with lipid metabolites. These results indicate that the abundance of the gut microbial taxa, especially the genera *Oscillibacter*, *Ruminiclostridium*, and *Negativibacillus* from the Ruminococcaceae family and the genus *Helicobacter*, is significantly correlated with lipid metabolites. Thus, *Helicobacter*, *Oscillibacter*, *Ruminiclostridium*, and *Negativibacillus* may be key microbial communities involved in alleviating lipid metabolism disorders.

4. Discussion

Natural dietary interventions that modulate the gut microbiome offer a promising strategy for combating obesity and related metabolic

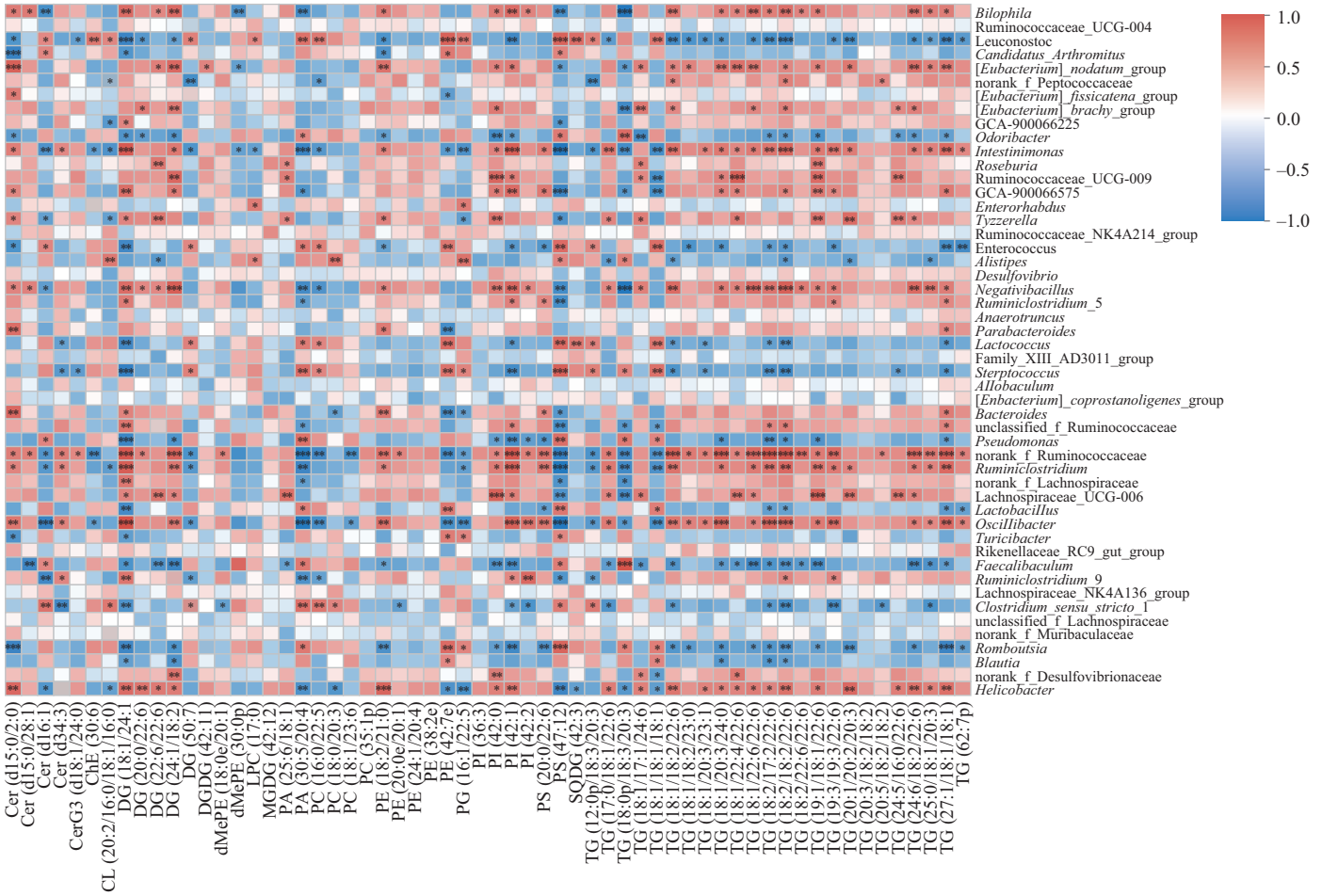

Fig. 7 Spearman correlation analysis of gut microbes and differential lipid metabolites. Top 50 differential microbes ranked by relative abundance. Top 60 differential lipid metabolites ranked by VIP. Significant differences were compared with each 2 groups, $*P < 0.05$, $**P < 0.01$, $***P < 0.001$.

diseases by correcting lipid metabolism. The chronic consumption of HFD poses a significant public health challenge, substantially elevating the risks of various metabolic disorders and associated healthcare burdens[23]. Characterized by excessive fat and energy intake, HFD promotes the pathological accumulation of lipids in the body, thereby instigating a cascade of metabolic disruptions. These include the destabilization of glycolipid homeostasis, dysregulation of the coagulation system, and functional impairment in multiple organs, notably the liver[24]. Increasing dietary fiber intake represents a well-established strategy to mitigate these adverse effects. Accordingly, this study investigates the therapeutic potential of ACA-DK, an insoluble dietary fiber derived from *A. camphorata* residue, to ameliorate HFD-induced dyslipidemia and its underlying metabolic disturbances. The underlying mechanisms were explored using an integrated lipid metabolomics and gut microbiota analysis.

Dietary fibers derived from different sources possess unique structural, chemical, and physicochemical attributes that confer several nutritional and health benefits[25]. Our findings demonstrate that the insoluble fungal fiber ACA-DK significantly alleviated HFD-induced dyslipidemia and gut dysbiosis. The efficacy of ACA-DK may be intrinsically linked to the unique properties of fungal-derived insoluble dietary fibers. Although often overlooked in favor of traditional sources, edible fungi are a rich reservoir of dietary fiber, with a characteristically high proportion of its content being the insoluble type[20-21]. This structural composition is critical to its function. Unlike soluble fibers that are extensively fermented in the proximal colon, insoluble fibers like ACA-DK undergo less degradation, allowing them to persist throughout the intestinal tract[26]. This persistence not only provides a sustained substrate for microbial production of short-chain fatty acids in distal gut regions but also crucially contributes to increased stool bulk and enhanced intestinal motility. We propose that the physical modulation of gut transit is a key mechanism by which ACA-DK remodels the gut microbiota and restores systemic lipid homeostasis. This hypothesis is supported by observed taxonomic shifts, including reductions in *Helicobacter* and Ruminococcaceae. Consequently, our findings highlight insoluble fungal fibers as a distinct and potent class of prebiotics worthy of further investigation. Notably, ACA-DK features a loose cellulose structure and demonstrates a direct regulatory effect on liver lipid metabolism, significantly reducing serum TG and TC levels. While, this study demonstrates the potent efficacy of ACA-DK, it is acknowledged that the absence of a middle dose and a positive control group are limitations. Future studies will incorporate these elements to precisely define the dose-response relationship and to directly benchmark ACA-DK's efficacy against standard therapeutics.

Our lipidomic analysis revealed that ACA-DK intervention significantly reversed the HFD-induced accumulation of key hepatic lipids, including TG, PC and PE (Fig. 3). This restorative effect aligns with the established understanding that HFD disrupts these

specific lipid pathways, as demonstrated by Mouskeftara et al.[27], who showed that such disruptions only gradually recover upon a return to a normal diet. Critically, our findings advance this understanding by demonstrating that ACA-DK supplementation, under a continued HFD, can actively mimic the beneficial restorative effect of dietary normalization.

Beyond simply reversing the quantity of these lipids, ACA-DK induced a qualitative improvement in their composition. A particularly noteworthy finding was the significant increase in highly unsaturated PC species. This shift is physiologically significant, as the acyl chain length and degree of PC unsaturation are crucial determinants of metabolic health, with HFD-induced pathologies being closely linked to deficiencies in such PC profiles[28]. Since PC plays a key role in regulating lipoprotein assembly and energy metabolism, its enrichment with highly unsaturated species likely represents a fundamental correction of HFD-induced metabolic dysfunction. Therefore, we propose that ACA-DK acts not merely by reducing fat absorption but by actively reprogramming hepatic glycerophospholipid metabolism. This targeted modulation, essential for maintaining membrane integrity and systemic lipid homeostasis, emerges as a central mechanism through which ACA-DK restores lipid balance, offering a novel therapeutic strategy against HFD-induced dyslipidemia[29-31]. In contrast to the established effects of other nutraceuticals on specific signaling pathways or lipid droplet dynamics, our findings highlight a novel role for insoluble fungal fiber in rectifying HFD-induced distortions in glycerophospholipid composition[32-33]. This unique metabolic action, coupled with its targeted suppression of pro-lipidemic gut microbes, distinguishes ACA-DK's mechanism of action in alleviating nonalcoholic fatty liver disease (NAFLD).

Lipid metabolites play a crucial role in the interaction between the brain-gut axis and the liver-gut axis. The gut microbiota influences lipid metabolism by responding to changes in nutrients such as carbohydrates and lipids in the environment[34]. An HFD, coupled with low dietary fiber, can disrupt the nutritional balance in the gut, thereby causing significant disturbances in the gut microbiota composition[35]. Dietary fiber substantially affects the gut microbiota[36]. The gut microbiota disruption caused by an HFD can be further transmitted to offspring during pregnancy[37]. Similar to the findings of Wang et al.[18], the HFD in our study increased the α-diversity of the gut microbiota and reduced the relative abundances of genera such as *Lactobacillus*, *Faecalibaculum*, and *Bifidobacterium*. However, ACA-DK supplementation caused no significant change in the α-diversity of the gut microbiota but non-significantly increased the relative abundance of *Lactobacillus*. This suggests that the effect of ACA-DK on the gut microbiota is different from that of water-soluble fibers.

The effect of an HFD on the gut microbiota also manifests as the proliferation of pro-inflammatory bacteria, leading to an increase in the levels of endotoxins such as lipopolysaccharide in the gut and destruction of the intestinal barrier[38-39]. An HFD substantially affects the abundance of the Ruminococcaceae family, which belongs to the Firmicutes phylum and plays a key role in maintaining the host's health[40]. However, different genera within this family may have vastly different effects in various diseases[41]. Sun et al.[42] showed that the polyphenol extract derived from the mushroom *Sarcodon leucopus* alleviated metabolic disorders in diet-induced obesity mice by reducing the abundance of Ruminococcaceae in the gut. Research has demonstrated that an HFD can significantly promote the relative abundances of genera such as *Oscillibacter*, *Negativibacillus*, and *Ruminococcus* from the Ruminococcaceae family, and that these genera are significantly positively correlated with blood lipid indicators[43-45]. In our study, consistent results were obtained, indicating that ACA-DK can effectively reverse the HFD-induced increase in the relative abundance of Ruminococcaceae.

Furthermore, we found that the relative abundance of *Helicobacter* was positively correlated with dyslipidemia. An HFD also tends to increase the relative abundance of *Helicobacter* in the gut[46]. Research has shown a clear synergistic effect between this genus and an HFD. *Helicobacter* infection can exacerbate metabolic disorders in HFD-fed mice by affecting host metabolism and promoting inflammation[47]. Our correlation analysis revealed that the HFD was closely associated with changes in the abundances of Ruminococcaceae and *Helicobacter*. ACA-DK supplementation significantly alleviated the HFD-induced gut microbiota dysbiosis, thereby improving lipid metabolism and reducing liver damage. The *Helicobacter*, *Oscillibacter*, *Ruminiclostridium*, and *Negativibacillus* genera may be key microbial groups involved in ameliorating dyslipidemia.

We emphasize that the difference between the Cur2 and Mod groups reflects a targeted action rather than a broad restructuring. The coordinated suppression of a network of bacteria associated with inflammation and increased lipid absorption (e.g., specific Ruminococcaceae members and *Helicobacter*) likely disrupts the pro-dyslipidemic microbial environment fostered by the HFD. This indicates that the modulation of the gut microbiota by ACA-DK is highly selective, and its lipid-improving effects are likely mediated primarily through the targeted suppression of specific harmful bacterial consortia rather than a broad promotion of all beneficial bacteria.

5. Conclusion

In conclusion, our study demonstrates that the insoluble fiber ACA-DK from *A. camphorata* effectively alleviates HFD-induced hyperlipidemia and hepatic steatosis. We have elucidated a novel dual mechanism: in the host, ACA-DK corrects glycerophospholipid metabolism; in the gut, it selectively targets and reduces pro-lipidemic microbes such as *Helicobacter* and Ruminococcaceae. The correlation between these microbial shifts and improved lipid profiles underscores the role of the gut-liver axis in ACA-DK's efficacy. Therefore, our work highlights ACA-DK not only as a promising functional food ingredient but also provides a mechanistic framework for the development of microbiota-directed therapies against metabolic diseases.

Declaration of competing interest

We declare that we have no conflict of interest.

Acknowledgments

This work was supported by the National Science Fund for Distinguished Young Scholars (32025029), the Natural Science Foundation of China (32272364), Shanghai Engineering Research Center of food microbiology program (19DZ2281100).

Appendix A. Supplementary data

Supplementary data associated with this article can be found, in the online version, at http://doi.org/10.26599/FSHW.2026.9250938.

References

[1] X. Li, D. Zhang, D.F. Vatner, et al., Mechanisms by which adiponectin reverses high fat diet-induced insulin resistance in mice, PNAS 117 (2020) 32584-32593. https://doi.org/10.1073/pnas.1922169117.

[2] Y. Wu, C.W. Wong, E.N. Chiles, et al., Glycerate from intestinal fructose metabolism induces islet cell damage and glucose intolerance, Cell Metab. 34 (2022) 1042-1053. https://doi.org/10.1016/j.cmet.2022.05.007.

[3] J.A. Wali, N. Jarzebska, D. Raubenheimer, et al., Cardio-metabolic effects of high-fat diets and their underlying mechanisms-a narrative review, Nutrients 12 (2020) 1505. https://doi.org/10.3390/nu12051505.

[4] M.M. Glavas, A.Y. Lee, I. Miao, et al., Developmental timing of high-fat diet exposure impacts glucose homeostasis in mice in a sex-specific manner, Diabetes 70 (2021) 2771-2784. https://doi.org/10.2337/db21-0310.

[5] D.I. Garcia, K.E. Hurst, A. Bradshaw, et al., High-Fat diet drives an aggressive pancreatic cancer phenotype, J. Surg. Res. 264 (2021) 163-172. https://doi.org/10.1016/j.jss.2020.10.007.

[6] Y. Tong, H. Gao, Q. Qi, et al., High fat diet, gut microbiome and gastrointestinal cancer, Theranostics 11 (2021) 5889-5910. https://doi.org/10.7150/thno.56157.

[7] K. Frazier, A. Kambal, E.A. Zale, et al., High-fat diet disrupts REG3γ and gut microbial rhythms promoting metabolic dysfunction, Cell Host Microbe 30 (2022) 809-823. https://doi.org/10.1016/j.chom.2022.03.030.

[8] L.K. Stenman, R. Holma, R. Korpela, High-fat-induced intestinal permeability dysfunction associated with altered fecal bile acids, World J. Gastroenterol. 18 (2012) 923-929. https://doi.org/10.3748/wjg.v18.i9.923.

[9] S.G. Mlodinow, M.K. Onysko, J.W. Vandiver, et al., Statin adverse effects: sorting out the evidence, J. Fam. Pract. 63 (2014) 497-506.

[10] F. Isken, S. Klaus, M. Osterhoff, et al., Effects of long-term soluble *vs*. insoluble dietary fiber intake on high-fat diet-induced obesity in C57BL/6J mice, J. Nutr. Biochem. 21 (2010) 278-284. https://doi.org/10.1016/j.jnutbio.2008.12.012.

[11] S. Chang, X. Cui, M. Guo, et al., Insoluble dietary fiber from pear pomace can prevent high-fat diet-induced obesity in rats mainly by improving the structure of the gut microbiota, J. Microbiol. Biotechnol. 27 (2017) 856-867. https://doi.org/10.4014/jmb.1610.10058.

[12] Q. Liu, J. Zhao, S. Liu, et al., Positive intervention of insoluble dietary fiber from defatted rice bran on hyperlipidemia in high fat diet fed rats, J. Food Sci. 86 (2021) 3964-3974. https://doi.org/10.1111/1750-3841.15812.

[13] A. Singla, O.P. Gupta, V. Sagwal, et al., Beta-glucan as a soluble dietary fiber source: origins, biosynthesis, extraction, purification, structural characteristics, bioavailability, biofunctional attributes, industrial utilization, and global trade, Nutrients 16 (2024) 900. https://doi.org/10.3390/nu16060900.

[14] B. Lyu, H. Wang, M.S. Swallah, et al., Structure, properties and potential bioactivities of high-purity insoluble fibre from soybean dregs (Okara), Food Chem. 364 (2021) 130402. https://doi.org/10.1016/j.foodchem.2021.130402.

[15] L. Yang, Y. Zhao, J. Huang, et al., Insoluble dietary fiber from soy hulls regulates the gut microbiota *in vitro* and increases the abundance of bifidobacteriales and lactobacillales, J. Food Sci. Technol. 57 (2019) 152-162. https://doi.org/10.1007/s13197-019-04041-9.

[16] S. Wang, J. Zhang, J. Li, et al., Label-free quantitative proteomics reveals the potential mechanisms of insoluble dietary fiber from okara in improving hepatic lipid metabolism of high-fat diet-induced mice, J. Proteomics 287 (2023) 104980. https://doi.org/10.1016/j.jprot.2023.104980.

[17] J. Yang, H. Wei, Y. Zhou, et al., High-Fat diet promotes colorectal tumorigenesis through modulating gut microbiota and metabolites, Gastroenterology 162 (2022) 135-149. https://doi.org/10.1053/j.gastro.2021.08.041.

[18] B. Wang, Q. Kong, X. Li, et al., A high-fat diet increases gut microbiota biodiversity and energy expenditure due to nutrient difference, Nutrients 12 (2020) 3197. https://doi.org/10.3390/nu12103197.

[19] J.F. Pierre, K.B. Martinez, H. Ye, et al., Activation of bile acid signaling improves metabolic phenotypes in high-fat diet-induced obese mice, Am. J. Physiol.-Gastrointestinal Liver Physiol. 311 (2016) G286-G304. https://doi.org/10.1152/ajpgi.00202.2016.

[20] P.C.K. Cheung, The nutritional and health benefits of mushrooms, Nutr. Bull. 35 (2010) 292-299. https://doi.org/10.1111/j.1467-3010.2010.01859.x.

[21] Y. Zhang, D. Wang, Y. Chen, et al., Healthy function and high valued utilization of edible fungi, Food Sci. Hum. Wellness 10 (2021) 408-420. https://doi.org/10.1016/j.fshw.2021.04.003.

[22] Y.J. Xia, P. Meng, S. Liu, et al., Structural and potential functional properties of alkali-extracted dietary fiber from *Antrodia camphorata*, Front. Microbiol. 13 (2022) 921164. https://doi.org/10.3389/fmicb.2022.921164.

[23] K.A. Posey, D.J. Clegg, R.L. Printz, et al., Hypothalamic proinflammatory lipid accumulation, inflammation, and insulin resistance in rats fed a high-fat diet, Am. J. Physiol.-Endocrinol. Metabol. 296 (2009) E1003-E1012. https://doi.org/10.1152/ajpendo.90377.2008.

[24] C.Y. Lian, Z.Z. Zhai, Z.F. Li, et al., High fat diet-triggered non-alcoholic fatty liver disease: a review of proposed mechanisms, Chemico-Biological Interactions 330 (2020) 109199. https://doi.org/10.1016/j.cbi.2020.109199.

[25] F. Guillon, M. Champ, Structural and physical properties of dietary fibres, and consequences of processing on human physiology, Food Res. Inter. 33 (2000) 233-245. https://doi.org/10.1016/s0963-9969(00)00038-7.

[26] Q. Ge, H. Li, Z. Zheng, et al., *In vitro* fecal fermentation characteristics of bamboo insoluble dietary fiber and its impacts on human gut microbiota, Food Res. Inter. 156 (2022) 111173. https://doi.org/10.1016/j.foodres.2022.111173.

[27] T. Mouskeftara, O. Deda, G. Papadopoulos, et al., Lipidomic analysis of liver and adipose tissue in a high-fat diet-induced non-alcoholic fatty liver disease mice model reveals alterations in lipid metabolism by weight loss and aerobic exercise, Molecules 29 (2024) 1494. https://doi.org/10.3390/molecules29071494.

[28] M. Nam, M.S. Choi, S. Jung, et al., Lipidomic profiling of liver tissue from obesity-prone and obesity-resistant mice fed a high fat diet, Sci. Rep. 5 (2015) 16984. https://doi.org/10.1038/srep16984.

[29] J. Yan, T. Horng, Lipid metabolism in regulation of macrophage functions, Trends Cell Biol. 30 (2020) 979-989. https://doi.org/10.1016/j.tcb.2020.09.006.

[30] H. Yoon, J.L. Shaw, M.C. Haigis, et al., Lipid metabolism in sickness and in health: emerging regulators of lipotoxicity, Mol. Cell 81 (2021) 3708-3730. https://doi.org/10.1016/j.molcel.2021.08.027.

[31] M. Suzuki, Regulation of lipid metabolism *via* a connection between the endoplasmic reticulum and lipid droplets, Anat. Sci. Int. 92 (2016) 50-54. https://doi.org/10.1007/s12565-016-0378-2.

[32] Y.F. Liu, N. Ling, B. Zhang, et al., Flavonoid-rich mulberry leaf extract modulate lipid metabolism, antioxidant capacity, and gut microbiota in high-fat diet-induced obesity: potential roles of FGF21 and SOCS2, Food Med. Homol. 1 (2024) 9420016. https://doi.org/10.26599/FMH.2024.9420016.

[33] L. Cao, Y. Wu, K.Y. Liu, et al., *Cornus officinalis* vinegar alters the gut microbiota, regulating lipid droplet changes in nonalcoholic fatty liver disease model mice, Food Med. Homol. 1 (2024) 9420002. https://doi.org/10.26599/FMH.2024.9420002.

[34] R. Caesar, V. Tremaroli, P. Kovatcheva-Datchary, et al., Crosstalk between gut microbiota and dietary lipids aggravates WAT inflammation through TLR signaling, Cell Metabol. 22 (2015) 658-668. https://doi.org/10.1016/j.cmet.2015.07.026.

[35] M.A. Hildebrandt, C. Hoffmann, S.A. Sherrill-Mix, et al., High-fat diet determines the composition of the murine gut microbiome independently of obesity, Gastroenterology 137 (2009) 1716-1724. https://doi.org/10.1053/j.gastro.2009.08.042.

[36] K.E. Morrison, E. Jašarević, C.D. Howard, et al., It's the fiber, not the fat: significant effects of dietary challenge on the gut microbiome, Microbiome 8 (2020) 15. https://doi.org/10.1186/s40168-020-0791-6.

[37] D.M. Chu, K.M. Antony, J. Ma, et al., The early infant gut microbiome varies in association with a maternal high-fat diet, Genome Med. 8 (2016) 77. https://doi.org/10.1186/s13073-016-0330-z.

[38] K.A. Kim, W. Gu, I.A. Lee, et al., High fat diet-induced gut microbiota exacerbates inflammation and obesity in mice *via* the TLR4 signaling pathway, PLoS ONE 7 (2012) e47713. https://doi.org/10.1371/journal.pone.0047713.

[39] J.R. Mujico, G.C. Baccan, A. Gheorghe, et al., Changes in gut microbiota due to supplemented fatty acids in diet-induced obese mice, British J. Nutr. 110 (2013) 711-720. https://doi.org/10.1017/s0007114512005612.

[40] J. Feng, H. Ma, Y. Huang, et al., et al., Ruminococcaceae_UCG-013 promotes obesity resistance in mice, Biomedicines 10 (2022) 3272. https://doi.org/10.3390/biomedicines10123272.

[41] C. Zhang, F. Chen, Y. Shen, et al., Sleep apnea is associated with the increase of certain genera of Ruminococcaceae and Lachnospiraceae in the gut microbiome of hypertensive patients, Exp. Rev. Respiratory Med. 16 (2022) 1247-1256. https://doi.org/10.1080/17476348.2022.2147509.

[42] L. Sun, L. Bao, D. Phurbu, et al., Amelioration of metabolic disorders by a mushroom-derived polyphenols correlates with the reduction of Ruminococcaceae in gut of DIO mice, Food Sci. Hum. Wellness 10 (2021) 442-451. https://doi.org/10.1016/j.fshw.2021.04.006.

[43] Y. Chen, M. Akhtar, Z. Ma, et al., Chicken cecal microbiota reduces abdominal fat deposition by regulating fat metabolism, NPJ Biofilms Microbio. 9 (2023) 8. https://doi.org/10.1038/s41522-023-00390-8.

[44] H. Luo, N. Ying, Q. Zhao, et al., A novel polysaccharide from *Rubus chingii* Hu unripe fruits: extraction optimization, structural characterization and amelioration of colonic inflammation and oxidative stress, Food Chem. 421 (2023) 136152. https://doi.org/10.1016/j.foodchem.2023.136152.

[45] Y.C. Tung, Z.R. Liang, M.J. Yang, et al., Oolong tea extract alleviates weight gain in high-fat diet-induced obese rats by regulating lipid metabolism and modulating gut microbiota, Food Funct. 13 (2022) 2846-2856. https://doi.org/10.1039/d1fo03356e.

[46] Q. Zhao, Z. Liu, Y. Zhu, et al., Cooked Adzuki bean reduces high-fat diet-induced body weight gain, ameliorates inflammation, and modulates intestinal homeostasis in mice, Front. Nutr. 9 (2022) 918696. https://doi.org/10.3389/fnut.2022.918696.

[47] A. Krupa, W. Gonciarz, P. Rusek-Wala, et al., *Helicobacter pylori* infection acts synergistically with a high-fat diet in the development of a proinflammatory and potentially proatherogenic endothelial cell environment in an experimental model, Inter. J. Mol. Sci. 22 (2021) 3394. https://doi.org/10.3390/ijms22073394.